

Reducing Wear of Steel Rolling Against Ti6Al4V Operating in Vacuum

Timothy L. Krantz*

Abstract

This work was motivated by a qualification test of a mechanism for a space telescope. During the test undesired wear debris was formed. In this project alternative materials and coatings were tested with intent to reduce wear and debris when steel has a misaligned rolling contact against Ti6Al4V. Testing was done using a vacuum roller rig mimicking the mechanism's contact conditions. Ten configurations were tested. Most configurations resulted in significant debris. A sputtered 1-micrometer-thick nanocomposite molybdenum disulfide (MoS₂) film provided the best wear protection. The best configuration made use of the MoS₂ coating on both materials, and in preparing for sputtering the anodized Ti6Al4V working surface was smoothed using an ultrasonic process.

Introduction

This work was motivated by results of a qualification test of a mechanism to be used for the James Webb Space Telescope. The mechanism is used to move a magnet for certain operations of the telescope's near infrared spectrograph (NIRSpec) instrument. The motion of the magnet is guided by a set of preloaded steel rollers in contact with anodized Ti6Al4V flat surfaces. The qualification testing was accomplished in a cold vacuum chamber to match as closely as possible the extreme deep space environment. Post-test inspections of the qualification test article revealed some wear of the steel rollers and mating Ti6Al4V surfaces, and some loose debris was found. The NASA Engineering Safety Center (NESC) investigated the potential risk of the wear and resulting debris to hinder the full capability of the NIRSpec instrument. This article describes results of roller tests of ten material configurations with the project intent to minimize wear debris.

Background – Qualification Test Article and Test Results

Following is a description of the qualification test article, test conditions, and results that motivated this research [1]. The mechanism of interest is a translator assembly that features a set of 11 rollers to guide the motion of a magnet (Figure 1). The translation of the magnet is used to control the positions of micro-shutters. The in-plane position is established by a set of four rollers contacting both sides of a guide rail defining the direction of motion. The out-of-plane position and motion is guided by a set of seven rollers. Three rollers are in contact with a base plate defining one plane and four rollers are in contact with a cover defining a second parallel plane. A motor and linkages provide the motive force. The translator assembly moves in a straight line for approximately 200 mm on each stroke. The translation time in one direction during testing was 10.5 seconds. The test duration was 96,000 forward and return motions.

Roller preload was established by a shimming procedure to provide a nominal normal load of 38 N. The roller profile was a circular crown with a flat feature superimposed on the center of the crown. Assuming line contact across the flat, the Hertz contact maximum pressure was 240 MPa. The rollers were machined from free machining 440F steel, annealed and passivated. Each roller was supported by a pair of deep groove ball bearings. The fastener securing the roller bearings to the axle was a locking style bolt assembled with a small amount of axial play. The rollers were in contact with Ti6Al4V that had been stress relieved and anodized.

* NASA Glenn Research Center, Cleveland, OH

After completion of the qualification test, wear was visible on the rollers of the translator assembly and on the mating surfaces. Figure 2 shows the condition of one qualification test roller. Some loose particulate debris was also found, which was collected and analyzed [1-2]. The worn surfaces and wear debris provide evidence that the wear process was primarily adhesive wear. In the net it appears that the steel has transferred to the mating Ti6Al4V surfaces. The loose wear debris included both the steel and titanium alloy materials. The severity of wear was not the same on all rollers.

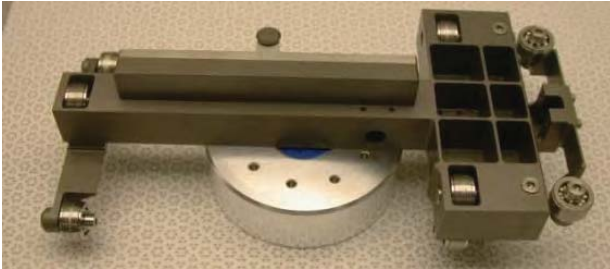


Figure 1. Translator Assembly [Ref. 1]

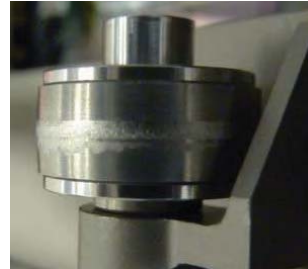


Figure 2. Condition of Roller After Completion of Qualification Test [Ref. 2]

The NASA Engineering and Safety Center (NESC) conducted an assessment to better understand the wear and provide recommendations that could reduce mission risk [3-4]. Experiments conducted by the NESC demonstrated that misalignment of a roller axis relative to the direction of travel is a key parameter influencing the propensity for wear. The NESC recommended two design changes for the rollers as follows. It was recommended that the roller material be changed from annealed 440F steel to 440C steel hardened to 58-60 Rockwell C. It was also recommended to change the roller profile geometry to eliminate the flat section superimposed in the center of the crown and to increase the crown radius. The NESC also recommended optimizing the assembly procedure to minimize roller misalignment.

The NESC has now completed additional work, reported herein, with goal to reduce mission risk from wear debris. There is little guidance in the open literature concerning detailed characterization of wear particles and transport of such particles. This is perhaps because for most applications small amounts of wear debris are of no consequence. The manufacture of semiconductors in a vacuum environment is one situation with similarity to the NIRSpec device in that high cleanliness is desired and wear particles can be of concern. For the manufacturing of semiconductors, proper bearing seals in combination with solid film lubrication has been proposed and studied to minimize adverse effects of wear debris [5]. The scope of the effort reported herein is evaluation of “alternative materials” for this mechanism. The words “alternative materials” includes coatings and solid lubrication films even if applied to the baseline substrate materials. For purposes on this study, it was assumed that the flight unit configuration would use a cover and baseplate made from anodized Ti6Al4V.

Laboratory Test Apparatus

Testing was done using the NASA Glenn Research Center Vacuum Roller Rig (VRR). Previous work has shown that the VRR can effectively simulate the mechanism contact conditions and wear phenomena [3,4]. The VRR data are also useful to supplement results of qualification tests. The rig allows for application and measurement of a load pressing the rollers together while having a purposely misaligned and adjustable shaft angle. The rig is depicted in schematic form in Figure 3. A drive motor provides motion to the driving roller. A second drive motor provides some motive power to the output roller to overcome bearing and seal friction. The output shaft roller is driven through a torque-limiting permanent magnet clutch. The clutch torque and the output shaft motor speed settings resulted in a net torque of 1 Nm through the output shaft and rolling slip of less than 2 percent. This closely approximates the mechanism rollers that are essentially free-rolling but with some support bearing and seal drag torque. The normal load pressing the rollers together is provided by an air cylinder. The cylinder acts through a pivot point to rotate the plate that mounts the driving shaft and drive motor in an arc motion. The pressure

to the cylinder, and thereby the load between the contacting rollers, is adjusted by a hand-operated valve (open-loop control). A turbomolecular pump assisted by a scroll pump provides vacuum in the test chamber. The typical condition in the test chamber is a pressure of about 4×10^{-5} Pa (3×10^{-7} torr). The most prevalent remaining constituent in the chamber during testing is water vapor as determined by residual gas analyzer [6]. The residual gas analyzer was used regularly to monitor the test chamber environment with no irregular results.

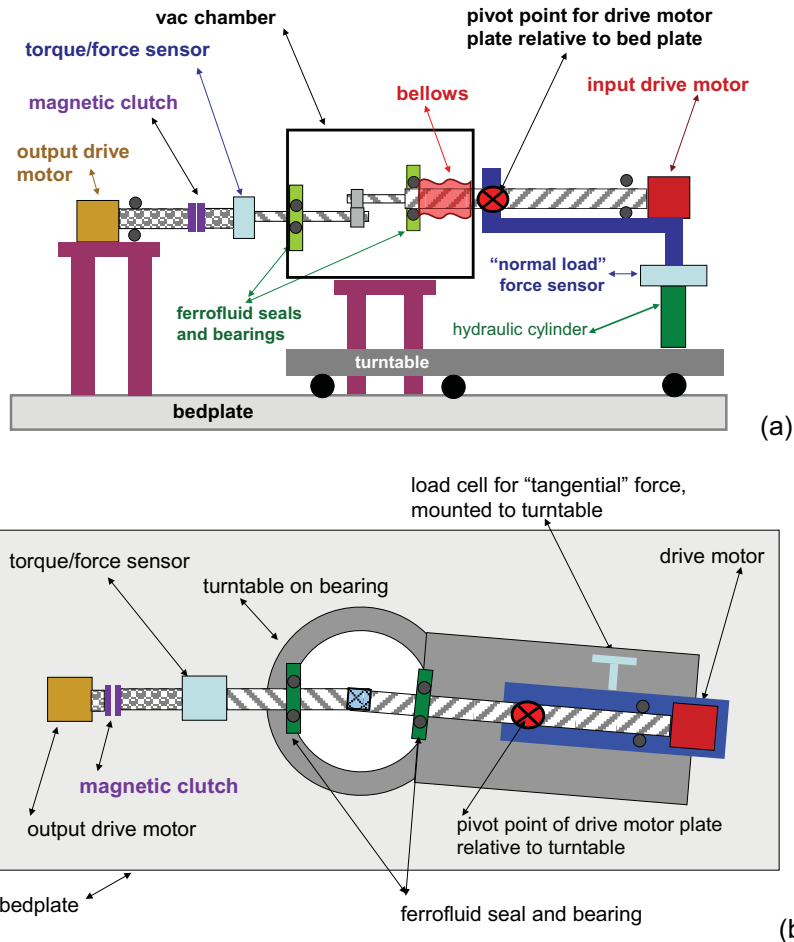


Figure 3. Schematic views of the vacuum roller rig. (a) Schematic, side view. (b) Schematic, overhead view with shaft misalignment depicted and exaggerated.

A set of sensors on the test apparatus monitors the test conditions. The outputs of the analog sensors were digitized at a rate of up to 0.66 Hertz. The misalignment of the driving roller shaft and driven roller shaft is depicted in an exaggerated manner in Figure 3. The misalignment is measured via a linear variable differential transformer (LVDT) attached to the bedplate. The LVDT tip moves against a stop on the turntable. To establish the aligned condition, special tooling blocks were machined to position the roller mounting surfaces as parallel to each other. The precision of this method for aligning is within 0.08 degree. The angular displacement from the aligned condition was calibrated by mounting a laser light source on the moving shaft at the roller mounting location and directing the light onto a paper placed at a known radial distance from the center of the turntable. The movement of the laser light was marked on the paper, and the distance between the points used to calculate the angular movement of the turntable and thereby relate this motion to the LVDT sensor output (voltage). The torque on the output shaft is monitored by a strain-gage torquemeter of 22 N-m (200 in lb) torque capacity. Calibration was done in place using deadweights on a torque arm. Figure 4 provides a schematic of the test roller setup labeled with some of the nomenclature used herein. The load pressing the rollers together is termed the "normal

load”. The normal load is applied via an air piston that acts through a load cell to move the drive motor plate that is pivot-mounted relative to the test chamber. Pressurizing the piston moves the input shaft in an arc motion toward the test roller. The arc motion is measured by an LVDT. Once the rollers are in contact, additional pressure to the air piston increases the normal load between the test rollers. Careful calibration processes allow calculating the test roller load using the sensor outputs from the load cell and the LVDT that measures the input shaft angular orientation [4]. Shaft speeds and total number of shaft revolutions were measured using encoders on each shaft. The encoder pulses were counted and recorded via a digital pulse counter. The encoders provide 6,000 pulses for each shaft revolution.

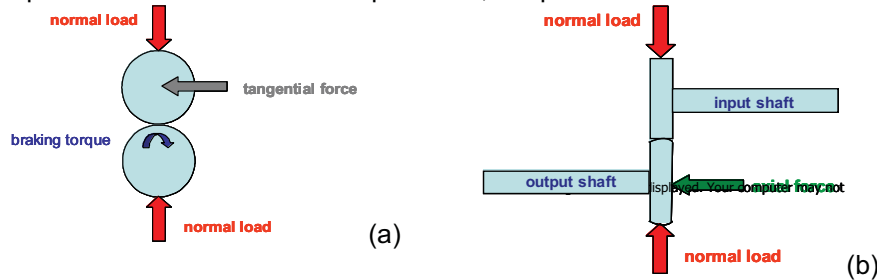


Figure 4. Simplified schematic view including some of the important sensed data. (a) Schematic, front view. (b) Schematic, side view.

When rollers operate in a misaligned condition, a force will develop in the direction of the shaft axis [7-10]. In such a condition points on the two rollers in intimate contact and within a “stick” zone of the contact patch are constrained to move in unison. If the points were not in contact the kinematic constraints would provide a slightly different path of motion. The difference in the actual path of motion and the motion that would occur if the points were not in contact gives rise to surface strains and a resultant axial force. A sensor to measure this force is labeled as the “axial force” sensor in Figure 4. The axial force sensor is co-located on the output shaft with the torquemeter.

The visual appearance of the test rollers were documented by digital photographs obtained through a viewport using a single-lens reflex camera with a 150-mm lens and a 12-million pixel image sensor. Wear debris was captured onto a flat rectangular pan located below the rollers. The analysis of such captured debris is beyond the scope of this article.

Contact Analyses and Test Conditions

Hertz contact analyses were completed to guide use of the VRR to best mimic the contact conditions of the NIRSspec mechanism. Results of the analyses were also used to guide selections of materials for evaluation. Although the actual contact conditions of rough surfaces differ from Hertz models that assume perfectly-smooth surfaces, the Hertz model solutions provide useful design indices. The Hertz contact solutions herein were produced using the approximate solution technique of Antoine, et al [11]. The mechanism makes use of steel rollers contacting a Ti6Al4V plane surface while the VRR tests a pair of rollers. The contact solutions for the mechanism are for roller geometry having a circular crown with 510-millimeter radius and with a 38-N (8.5-lbf) normal load pressing the steel roller to the Ti6Al4V plane. Contact solutions for VRR are for a normal load of 130 N (30 lbf) pressing the two rollers together. The VRR rollers are 35.6-mm outer diameter, the upper roller has a circular crown of 400 mm, and the lower roller has a flat profile. The Hertz contact condition solutions are summarized in Table 1. The contact ellipses are short in the rolling direction (labeled “b” in the diagram contained in the table) and have similar aspect ratios, 14.3 for the mechanism and 11.3 for the VRR. The contact ellipse is somewhat larger for the VRR because of the larger diameters of the VRR rollers. The contact pressure magnitudes are somewhat larger in the VRR, approximately 40% larger comparing the maximum contact pressures. Use of a lower normal load in the VRR would have provided a closer match of the contact conditions, but because of VRR constraints the 130-N load was used for the experiments.

The misalignment of the roller rotation axis relative to the actual direction of rolling motion is an important parameter influencing the wear rates. In this work the VRR was operated with misalignment angle of 0.9 degree as such misalignment had produced relevant wear phenomena in previous work [3,4]. The sliding distance that promotes wear of slightly misaligned rollers may be approximated as proportional to the product of misalignment angle and the width of the contact region. This approximate sliding distance concept is depicted in Figure 5. The approximate sliding distance per contact pass was 3.1 micrometer for the VRR. If operating at the same misalignment angle of 0.9 degree the approximate sliding distance per contact pass for the mechanism would be 1.9 micrometer. The speed of the test rig was 20 revolutions per minute. The speed was selected to provide a contact passing time of same order as the mechanism but the test was operated with a slightly faster rate to obtain the desired number of contact passes in practical calendar time. The contact passing times were 0.009 second for the mechanism and 0.005 second for the VRR tests.

There was no single VRR test duration that could mimic the duration needed for the mechanism. The VRR makes use of equally sized rollers and so VRR roller surfaces experience equal number of contact pass cycles per unit of time. For the mechanism, the steel rollers and titanium-alloy planes have differing numbers of contact cycles. Using 48,000 actuations of the mechanism as the needed life, with each actuation requiring a forward and reverse traverse, the duration for some points on the mechanism's titanium-alloy plate is 96,000 contact cycles. Other points of the mechanism's plate are passed over by two rollers for each traverse, requiring 192,000 contact cycles. The mechanism steel roller surfaces experience up to three contact cycles per traverse, requiring 288,000 contact cycles. Further complicating selection of the VRR test duration, the lifetime of a solid lubricating film is not reliably calculated for all situations by simple proportionality to contact cycles. For mild wear, the wear rate is often modeled, to a first approximation, using the Archard wear model [12] as proportional to the product of contact pressure and sliding distance. The VRR test duration was selected as 90,000 contact cycles. This selection enabled a desired testing pace of two tests per week and was considered to provide a reasonable match of both total contact cycles and a simple wear index (product of sliding distance and contact pressure) in comparing the VRR to the mechanism. Table 2 summarizes some of the key engineering parameters one might use to compare VRR to the mechanism in terms of contact conditions and durability concepts. The VRR can be considered as an accelerated wear test in terms of higher contact pressures and faster speeds. In this way the alternative materials were evaluated on a relative basis with good relevance to the application. The VRR tests were intended to complement but not substitute for qualification testing.

Table 1. Hertz Contact Conditions

	mechanism	test rig
pressure, max. (MPa)	330	460
pressure, mean (MPa)	220	310
a (mm)	1.77	2.30
b (mm)	0.124	0.200
aspect ratio, a/b	14.3	11.3

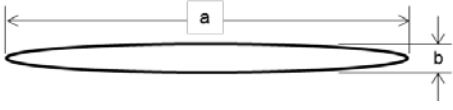



Figure 5. Approximate model of sliding distance of a misaligned roller contact. (a) Elliptical contact ellipse of width R, misalignment angle t , and actual rolling path R' . (b) Approximate sliding distance $S \approx R \cdot \tan(\tau) \approx R \cdot \tau$.

Table 2 – Comparison of the Test Rig and Mechanism Contact and Durability Metrics

	VRR	mechanism		
		steel roller	Ti6Al4V, two rollers, same track	Ti6Al4V, one roller only in track
duration, contact passes	90,000	288,000	192,000	96,000
wear index (Pa·m/10E6) ^a	86	120	80	40
pressure, max (MPa)	460	330		
rolling speed (mm/sec)	37.2	13.3		
contact passing time (sec)	0.005	0.009		

^a wear index defined as product of mean of Hertz pressure-sliding distance-number of contact passes for 0.9-degree misalignment angle for both system per the approximate sliding distance concept of Figure 5.

Selections of Alternative Materials and Configurations

A set of potential alternative materials were selected based on study of the literature, discussions with experts in the field, and implementation constraints. Liquid lubrication was not considered because of the extreme cold temperature of this application. Two review papers provide direct guidance and a substantial listing of relevant solid lubrication information [13,14]. Five different fundamental alternative material candidate solutions were selected for evaluation, as follows:

1. Use of polyimide rollers rather than steel rollers. Such material has been used for space applications and has been proposed for use as traction rollers. The experiment made use of a readily available VRR roller made from an unfilled base polyimide resin [15].
2. Use of a bonded, PTFE-type solid lubricant coating on the steel roller. The binder was an inorganic type with highest available strength.
3. Use of an alternative surface treatment to the currently employed anodizing treatment of the Ti6Al4V material, with intent to provide an adherent, hard, wear resistant layer of oxides. The selected treatment of the Ti6Al4V was a plasma electrolytic oxidation process [16].
4. Use of metal-doped diamond-like carbon coatings applied one or both surfaces to provide an adherent layer of high hardness and toughness. Some success has been reported for this approach for prevention of cold welding of Ti6Al4V in vacuum [17]. Such an approach has also been reported to improve durability of oil-lubricated bearings under certain operating conditions [18]. Two such coatings were selected, one a (TiC)_aC:H type and one a (WC)_aC:H type. The coatings were applied by physical vapor deposition.
5. Use of a molybdenum-disulfide (MoS₂) type sputtered solid lubricant film applied to one or both contacting surfaces. The selected film is a nanocomposite coating with composition including antimony oxide and gold. Such compositions have been studied by others for use in vacuum conditions [19]. MoS₂ has an extensive heritage as an effective solid lubricant for cold vacuum conditions. The coating thickness was intended to be 1 micrometer.

The material configurations selected for testing evolved as test results were obtained. Ten configurations were tested as listed in Table 3.

Table 3 – Tested VRR roller-pair configurations.

Configuration	Upper roller	Lower roller
1	440F ; annealed ; passivated	Ti6Al4V ; anodized
2	440C ; hardened ; passivated	Ti6Al4V ; anodized
3	polyimide	Ti6Al4V ; anodized
4	440C ; hardened ; passivated; bonded PTFE solid lube	Ti6Al4V ; anodized
5	440C ; hardened ; passivated	Ti6Al4V ; PEO; bonded solid lube
6	440C ; hardened ; passivated	Ti6Al4V ; (WC)aC:H DLC
7	440C ; hardened ; (TiC)aC:H DLC	Ti6Al4V; (TiC)aC:H DLC
8	440C ; hardened ; passivated ; nanocomposite MoS ₂	Ti6Al4V ; anodized
9	440C ; hardened ; passivated ; nanocomposite MoS ₂	Ti6Al4V ; anodized; nanocomposite MoS ₂
10	440C ; hardened ; passivated ; nanocomposite MoS ₂	Ti6Al4V ; anodized;ultrasonic smoothing nanocomposite MoS ₂

Experiment Procedures and Results

Experiment Procedures

The upper roller material for one test was made was polyimide material, otherwise the upper roller was 440 steel. The upper roller in all cases had a 400-mm crown radius and had a width of 13 mm. The lower roller for all testing was made from Ti6Al4V, had a flat profile, and had a width of 16.5 mm. Rollers were tested in a “tribologically clean” condition. For cases of rollers that had a coating by sputtering or physical vapor deposition, the rollers were stored in vacuum-sealed bags immediately following deposition and then were opened just prior to installation, and so special cleaning was not required. For cases of rollers with hard surfaces, rollers were scrubbed using 0.05-micron alumina powder suspended in deionized water. After appropriate scrubbing the roller was rinsed in deionized and filtered water. The cleaning procedure was different for the cases of the polyimide roller and the roller with the bonded type lubricant film. Alumina powder was not used to avoid possibility to imbed the powder into the relatively soft materials. In these cases, the rollers were cleaned using isopropanol rinse followed by ultrasonic cleaning in deionized water. It was confirmed that surfaces were clean of all oils by checking for uniform and full wetting of the surfaces. Water was then removed using dry, pressurized nitrogen. Once cleaned, the rollers were handled only with gloved hands and were transported to the rig using closed glass jars.

Just prior to installation, the surface textures of rollers were documented by tracing with a stylus profilometer using a 2-micrometer-radius conisphere-tipped stylus. Traces were recorded in the both circumferential (rolling) direction and in the profile (axial) direction. The final step prior to installing rollers into the test chamber was to measure the mass using a scale with 0.0001 gram resolution. After installing the rollers onto the test shafts, the hinged chamber door was immediately closed and the vacuum system operated to bring the chamber to a partial pressure of 6.7 Pa (50×10^{-3} torr) within one minute. The test chamber was then brought to a pressure of 1×10^{-3} Pa (7.5×10^{-6} torr) or less before beginning testing of the rollers. Roller mass and stylus profilometer data were obtained after testing.

Experiment Results

Following is a discussion of the roller wear test results. The information is organized to aid the discussion. The order of the discussion does not match chronological order of testing. The experimental data to be discussed herein includes the visual appearance of the roller surfaces as testing progressed, amounts of visible wear debris, the change of mass of rollers both individually and as a pair, and roller surfaces conditions at start and end of test as revealed by stylus profilometer measurements.

Configuration 1 – Results: The first configuration for discussion is the upper roller 440 F steel, annealed and passivated and the lower roller material Ti6Al4V, anodized. This configuration matches that of a tested qualification unit [1,2]. A motivation for this test was to demonstrate that the test conditions selected for this work (i.e. the speed, load, misalignment angle, and duration) would produce the relevant wear phenomena. One test was completed using this configuration. Significant adhesive wear and plastic flow of material occurred throughout the test. After 78,000 cycles high vibrations were occurring, and the test was stopped early of the targeted 90,000 cycles to avoid damage to the apparatus. The final roller conditions for this test are provided in Figure 6(a). The upper steel roller lost 0.0710 g mass while the lower Ti6Al4V roller gained 0.059 g mass. As a pair the rollers lost 0.011 g mass. Stylus profile inspections of the tested upper roller revealed a material peak along one edge of the contact, likely from plastic flow, reaching over 100 micrometer heights. Similar inspection of the tested lower roller revealed added material in the contact region reached 60 micrometer of height. This test confirmed that the operating conditions selected for this study reproduced the relevant wear phenomena of the qualification test unit.

Configuration 2 – Results: The second configuration for discussion is the upper roller 440 C steel hardened to HRC 58-60 and passivated and the lower roller anodized Ti6Al4V. The three tests completed using this configuration all had similar wear behavior. Significant adhesive wear had occurred after 25 percent of the test duration. The final conditions of the rollers featured distinctive worn surface topographies and significant adhesive wear had occurred; see Figure 6(b). From profilometer inspections the steel roller wear valleys had typical depths of 15 micrometers. The Ti6Al4V roller had a region with material removed and just adjacent another region with material added. Mass measurements confirmed that in the net the steel rollers lost mass and Ti6Al4V rollers gained mass. The sizes of the valley features of the steel roller and the peak features of the Ti6Al4V roller for this configuration were of smaller magnitudes by a factor of two to three as compared to Configuration 1. This result is consistent with the general trends observed in the earlier NESC study [3-4] that had quantified wear rates being less by order of two to three for hardened 440C rollers compared to annealed 440 F rollers.

Configuration 3 – Results: The third configuration for discussion comprises one test with the upper roller material polyimide and the lower roller anodized Ti6Al4V. The lower anodized roller abraded the upper polyimide roller like a machining process. The test created a great amount of polyimide debris [Figure 6(c)], and the test was stopped after 38,000 cycles far short of the intended 90,000 cycle duration. After cleaning with a soft-bristle brush, rollers look almost like the new condition. This material configuration might be suitable for situations where the polyimide wear debris could be tolerated, but it is not suited for the present application.

Configuration 4 – Results: The fourth configuration for discussion is the upper roller material of hardened and passivated 440C steel with a solid lubricant bonded film. The bonded film was a commercially available PTFE type with an inorganic binder. The product vendor considered the mean test pressure as “uncomfortably close to” the binder strength limit. The lower roller material was anodized Ti6Al4V. One test comprising 83,000 cycles of this configuration was completed. The bonded film was abraded and worn away by the anodized surface of the lower roller. A great volume of powdery debris was formed and transported toward one edge of the roller contact by the sweeping action of the misaligned rollers [Figure 6(d)]. Once the bonded film was compromised, adhesive wear occurred with similar wear rate of uncoated rollers. It appears that the binder strength was indeed insufficient, per the concerns expressed by the product provider. This configuration is obviously not suited for the present application.

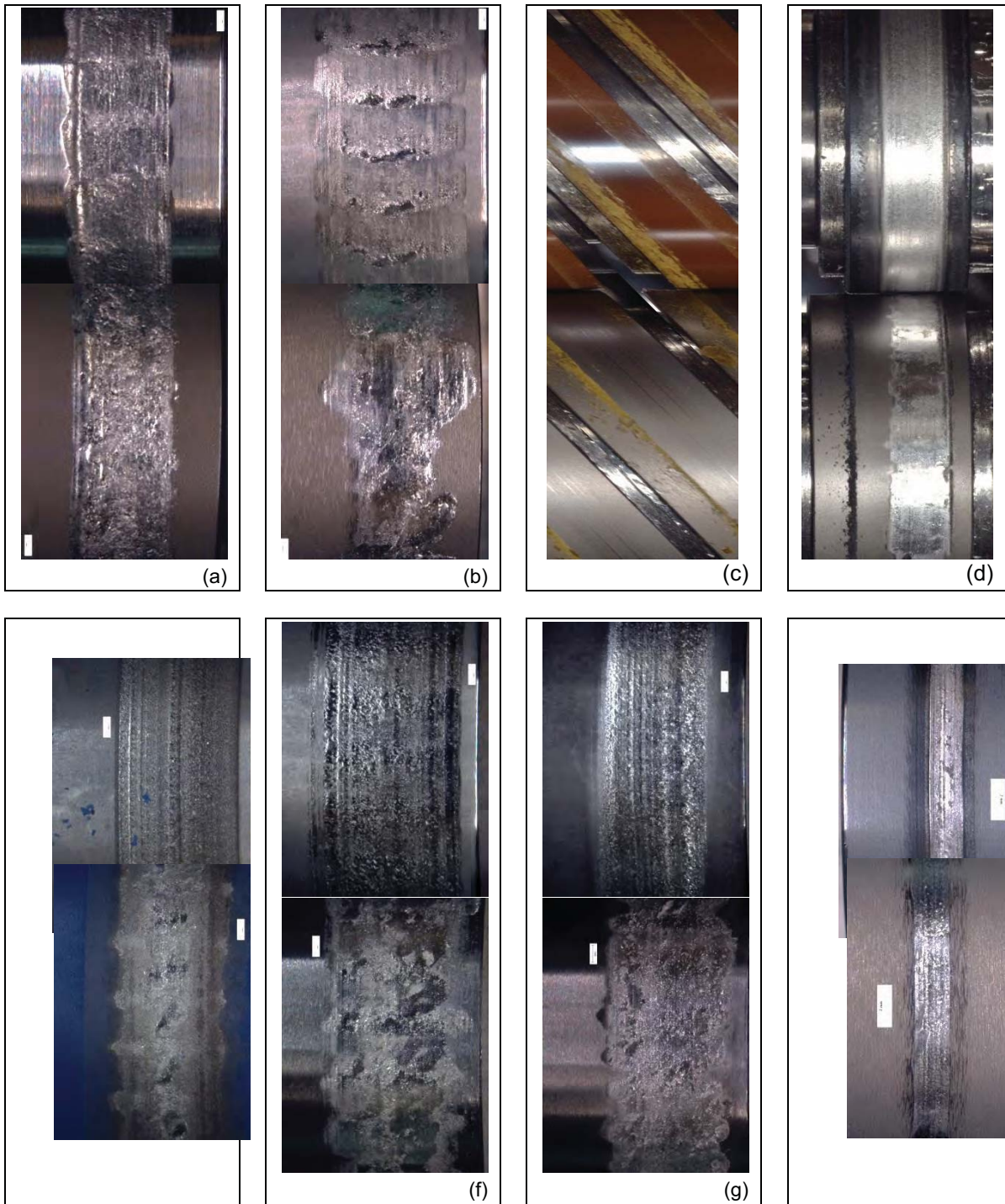


Figure 6. Conditions of rollers at end of test.
(a) Config. 1, annealed 440F steel. (b) Config. 2, hardened 440C steel.
(c) Config. 3, polyimide upper roller.
(d) Config. 4, bonded film.
(e) Config. 5, PEO of Ti6AL4V.
(f) Config. 6, lower roller coated with (WC)aC:H
(g) Config. 7, both rollers coated with (TiC)aC:H.
(h) Config. 8, upper roller coated with nanocomposite MoS₂

Configuration 5 – Results: The fifth configuration for discussion is the upper roller material hardened and passivated 440C steel. The lower roller was Ti6Al4V material treated by plasma electrolytic oxidation (PEO). The vendor of the PEO process also chose to apply on top of the PEO treated surface a bonded solid lubricant film, a combination that in their experience performed well. The configuration was put to test with the philosophy that failure of the bonded film need not define the capability of the PEO surface itself. One 93,000 cycle test was completed. The blue-colored solid lubricant film wore away and created a mixture of powder and large flakes of debris. The blue-colored bonded film transferred onto the upper steel roller during the early part of the testing, but later this transferred film was almost completely removed from the upper roller [Figure 6(e)]. There was significant adhesive wear. The final condition of the rollers for this configuration appeared visually similar to that of Configuration 2. The net mass lost from the upper 440C roller was 0.002 gram, also similar to the result of Configuration 2. Given the result of this test and given the lack of experience using the PEO process for space mechanisms, it was decided not to further pursue evaluations of PEO-treated Ti6Al4V for this application.

Configuration 6 – Results: The sixth configuration for discussion is the upper roller material hardened and passivated 440C steel and the lower roller material Ti6Al4V with a PVD-applied coating of a (Wc)aC:H diamond-like-carbon (DLC) composition. One test was completed to 91,000 cycles. In this test configuration the problematic Ti6Al4V alloy was coated with a galling-resistant composition hoping to defeat the adhesive wear mechanism. However, for these particular contact conditions wear occurred to both rollers throughout the course of the test. As the wear occurred a significant amount of debris was noted on the debris tray. During the first 25 percent of the test duration, the rollers surfaces appeared to have relatively low surface roughness suggestive of abrasive wear. By the end of the test the rollers surfaces conditions suggested the process had become primarily adhesive wear [Figure 6(f)]. Profilometer inspections of the rollers confirmed that the wear behavior of this configuration was different from the other configurations. The lower Ti6Al4V roller had a prominent wear valley with roughness features within the wear region, and by mass measurements the lower roller net mass lost was 0.007 gram. This was the only configuration where the majority of mass loss was only from the lower Ti6Al4V roller. This configuration is not suited for the present application.

Configuration 7 – Results: The seventh configuration for discussion is the upper roller material of hardened 440C steel and the lower roller Ti6Al4V. The surfaces of both rollers were coated with a (TiC)aC:H DLC composition applied by PVD. One test was completed to 96,000 cycles. The wear progression had some similarities to the test of configuration 6. Wear occurred to both rollers throughout the course of the test. As the wear occurred, a significant amount of debris was noted on the debris tray. Early in the test the wear may have been abrasive wear, but as the test progressed the surface roughness features became more apparent and end of test conditions suggested adhesive wear [Figure 6(g)]. Profilometer inspections of the rollers at the end of test show differing behaviors for Configuration 6 (lower roller only coated) compared to Configuration 7 (both rollers coated). The (Wc)aC:H coated lower roller of configuration 6 that was mated to an uncoated upper roller had no peak features and one prominent wear valley. On the other hand, for configuration 7 with (TiC)aC:H coating on both rollers, the lower roller had both peak and valley features. The upper rollers for Configurations 6 and 7 have similar surface profiles at the end of the test having a combination of peak and valley features of about 5 micrometer size. The use of the DLC coatings changed the wear behavior compared to tests without any coatings or solid-film lubrication. While DLC coatings may have a place for space mechanisms with more optimization and research, further consideration and testing of DLC coatings was not pursued for this application.

Configuration 8 – Results: The eighth configuration for discussion is the upper roller material hardened 440C steel and the lower roller anodized Ti6Al4V. The upper roller only was provided a MoS₂ nanocomposite coating by PVD sputtering. Four tests were completed using this configuration. The steel upper rollers with the sputtered coatings were passivated prior to coating except for one test the roller was not passivated because of testing schedule. The lack of passivation for one test probably did not have a big influence on performance, as the rollers are processed by a high-energy ion beam just prior to sputtering. The ion beam likely removes most or all of the oxides created during passivation. The test

durations ranged from 90,000 to 97,000 cycles. The wear behavior was not fully consistent for this set of four tests. In two cases there was moderate wear by the end of test. For these two tests the steel rollers lost mass and the Ti6Al4V rollers gained nearly equal mass. The mass change was of the order 0.020 gram for each roller of the two tests having moderate wear. For the other two tests with minor wear, the roller mass changes were nearly an order of magnitude less compared to the two tests with moderate wear. The photograph of Figure 6(h) shows a representative end-of-test condition for this configuration. Considering the four tests of this configuration as one grouping, the adhesive wear phenomenon was delayed and the overall wear rate was reduced as compared to tests without a solid lubricant film.

The reasons for the differing behaviors of the four tests of this configuration have not been determined conclusively. For one of the two tests with moderate wear, the coating thickness was about one-half of the intended thickness because of a temporary problem with the coating process. The thinner film was likely at least partially responsible for the less effective wear protection. From scanning-electron microscope inspections, for the other test with moderate wear, little transfer of sputtered film to the mating roller was observed. However, significant transfer did occur for a test that resulted in better wear protection. The reason for the lack of film transfer has not been determined. The scanning-electron microscope inspections revealed trace organics on some rollers from this configuration, and the likely source was a temporary coating-equipment problem. It is possible that the trace organics could have interfered with the solid lubricant film-transfer process, but this speculation is uncertain as trace organics and film transfer was found together for one of the low-wear cases from this configuration.

During a fifth test of this configuration, a mechanical failure of a rig part prevented rotation of the lower roller. The rollers operated in rolling condition for approximately 7,000 cycles, then ran unattended for an additional 47,000 revolutions of the upper roller with the lower roller stalled, not rotating. Although the full sliding does not represent the relevant contact conditions, the result is included herein as one that was quite striking. The final conditions of the test rollers showed some minor wear and perhaps some compromise of the MoS₂ coating, but large-scale adhesive wear was prevented (Figure 7). This test demonstrated effective wear protection. One can consider that once the lower roller stalled, a very small distance on the uncoated lower roller was in contact with a long distance of coated surface on the upper roller, the ratio being about 140:1. This experience illustrates the difficulty of extrapolating tribology test results from pin-on-disk or block-on-ring configurations of pure sliding to a different type of rolling-sliding contact condition. Still, this test produced evidence that the selected coating system is one that can provide effective wear protection in vacuum. The words “coating system” here indicates both the coating elemental composition and the process for coating application.

Configuration 9 – Results: The ninth configuration for discussion used the same nanocomposite MoS₂ coating as was used for Configuration 8, but in this configuration both rollers were coated. The upper roller substrate was passivated, hardened 440C steel. The lower roller substrate was anodized Ti6Al4V. Two tests of this configuration were completed, for 93,000 and 90,000 cycles, respectively. The test results for these two tests were consistent with good wear protection demonstrated. After some running-in of the surfaces, the underlying surface texture of the upper roller became visible. The lower roller surfaces developed a reflective sheen texture [Figure 8(a)]. All rollers lost some mass; none gained net mass by adhesive wear of the mate as occurred for uncoated roller pairs. The masses lost were small, less than 0.0003 gram mass lost per roller. From these visual assessments the wear protection was judged as excellent. However, the debris pans of these tests had a significant number of bright particles that were reflecting light and easy to see without aid of magnification. Profilometer inspections showed essentially no wear on the upper roller. Inspection also revealed a wear valley of about 2 to 3 micrometer depth on the lower roller [(Figures 8(b-c)]. Although this configuration prevented large-scale adhesive wear, the debris released from the lower roller was still significant, and such debris could pose some mission risk.

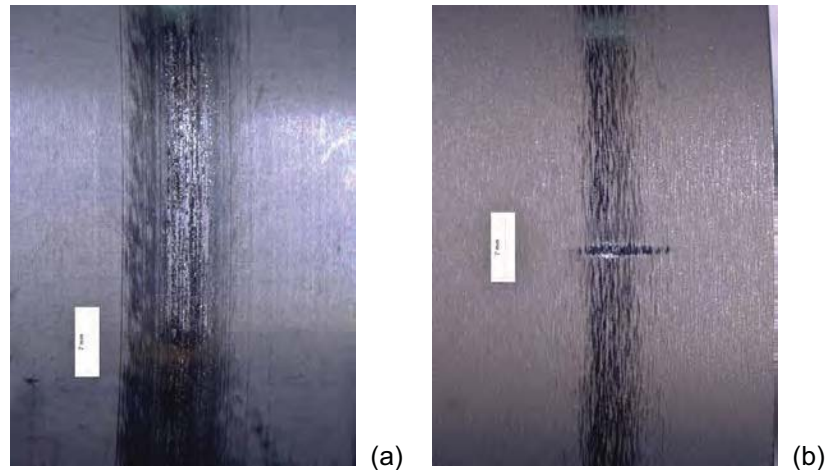


Figure 7 – Conditions of rollers at end of test from an unintended but interesting full sliding test. (a) Upper MoS₂ nanocomposite coated roller. (b) Uncoated lower roller, stalled member.

Configuration 10 – Results: The tenth and final configuration for discussion was almost identical to Configuration 9, except there was one additional processing step by the vendor in preparing Ti6Al4V rollers for sputtering. The nanocomposite MoS₂ coating was present on both upper and lower rollers for this configuration. It was noticed that the anodized surface of the titanium alloy rollers were quite rough, and roughness of such magnitude was judged as not favorable for minimizing wear. The lower titanium-alloy roller surfaces were smoothed by directing ultrasonic energy to the surfaces using a hand held probe. Aside from this added “smoothing” step for the anodized Ti6Al4V rollers that was done just prior to application of the coating, Configurations 9 and 10 were otherwise identical. Six tests were conducted for this configuration to more than 87,800 cycles for each test. Four of the tests provided excellent wear protection. Two of the tests, while slightly lesser performing, still provided very good wear protection. For one of the two lesser performing tests, the coating thickness was about one-half of the intended thickness because of a temporary problem with the coating process. The thinner film was likely at least partially responsible for the less effective wear protection. For the other lesser-performing test, a narrow wear track developed after about 60,000 cycles covering about one-third of the contact width. The photograph of Figure 9 shows typical end-of-test conditions of the rollers for the four tests that provided excellent wear protection.

Profilometer inspections showed essentially no wear, to the precision that could be measured by the stylus inspection technique, for both rollers. Typical lower roller inspections at start and end of test are provided in Figure 9(b-c). The undetectable wear on the lower roller is in quite contrast to the behavior of Configuration 9, per Figure 8(c) whereby a distinct wear valley was produced. It is interesting that the asperity features within the wear track of Figure 8(c) are very similar in shape and magnitude to the asperity features of the ultrasonically-smoothed and coated, but untested, roller of Figure 9(b). The many bright particles of debris easily seen without magnification on the debris pan during tests of Configuration 9 were absent during all tests of Configuration 10. Comparing the profilometer inspections of the lower rollers before test shows the effect of the ultrasonic smoothing process. Without the ultrasonic smoothing, the surface has asperities with high slopes as had resulted from the anodizing process. The asperity peaks are removed and/or deformed by the ultrasonic smoothing process [compare Figure 8(b) to Figure 9(b)] providing a more favorable surface for avoiding wear.

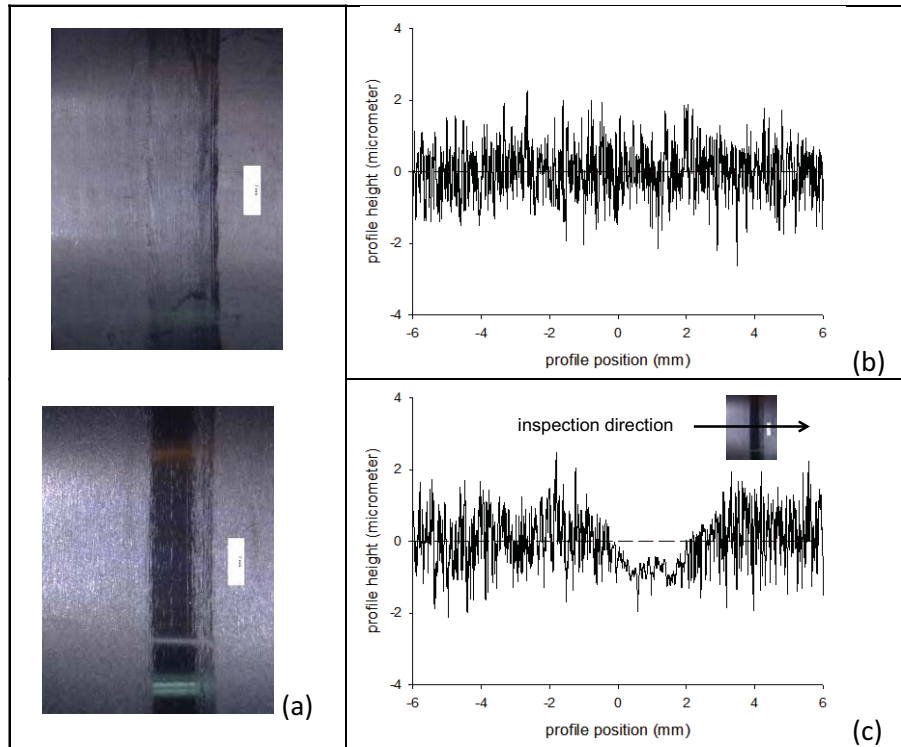


Figure 8 – Data from Configuration 9. (a) Conditions of rollers, end of test. (b) Profilometer inspection, lower roller, start of test. (c) Profilometer inspection, lower roller, end of test.

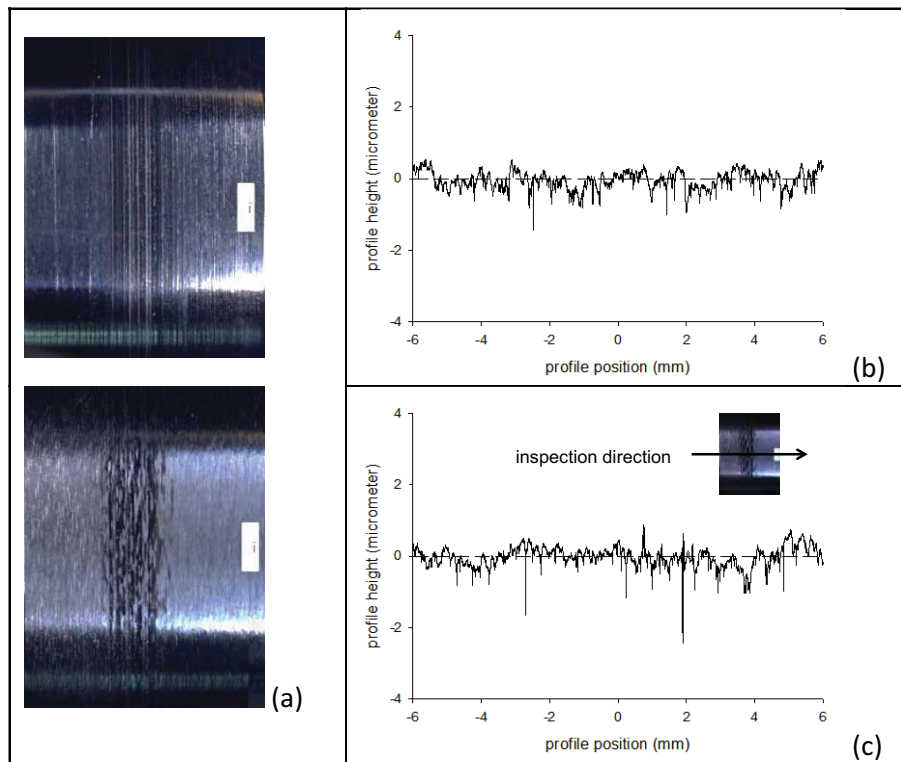


Figure 9 – Data from Configuration 10. (a) Conditions of rollers, end of test. (b) Profilometer inspection, lower roller, start of test. (c) Profilometer inspection, lower roller, end of test.

Configuration 10 provided the best wear protection and least amount of visible wear debris of all configurations tested. This conclusion is supported each and every aspect of the experimental data, that is: (1) excellent wear protection per qualitative assessment of the roller surface conditions; (2) low mass loss for both rollers, (3) wear depths were too small to be detected by profilometer inspection. It is recommended that this configuration should be carefully considered for implementation including durability and performance evaluations of the mechanism subsystem in appropriate cold-vacuum conditions.

Summary

After a qualification test of a mechanism for a space telescope, roller wear and particulate debris from adhesive wear was noted. With intent to minimize wear and resulting debris, sets of experiments were completed using a vacuum roller rig to mimic the mechanism contact conditions. Ten configurations were tested. The roller-pair material configurations were evaluated on basis of qualitative assessment of roller surface conditions, mass lost or gained by each roller, and wear phenomena as could be assessed by stylus profilometer and scanning-electron-microscope inspections. Specific findings were:

1. Changing the roller material from annealed 440F steel to 440C steel hardened to HRC 58-60 resulted in a reduction of overall wear by a factor of two to three.
2. Use of a polyimide roller instead of a steel roller is not suited for this application as the anodized Ti6Al4V surface created polyimide debris in a manner like a machining process.
3. The bonded solid lubricant film that was applied to the steel roller was abraded and/or broke down from the contact pressure. Large amounts of debris were created.
4. While diamond-like-carbon coatings altered the wear behavior, large amounts of debris were created. The investigated diamond-like-carbon coatings are not suited for this application.
5. Application of a nanocomposite MoS₂ film significantly reduced the wear and production of wear debris.
6. Application of the nanocomposite MoS₂ film to both rollers provided better wear protection than providing the coating to the upper hardened 440C steel roller only.
7. Smoothing of the anodized Ti6Al4V prior to coating with the nanocomposite MoS₂ film resulted in better wear protection and the least amount of visible debris.
8. It is recommended that Configuration 10 should be carefully considered for implementation. Configuration 10 is use of a nanocomposite MoS₂ film sputtered on passivated 440C steel hardened to HRC 58-60 and also sputtered on anodized Ti6Al4V that has been ultrasonically smoothed after anodizing and prior to sputtering.

Acknowledgements

This research was initiated and supported by the NASA Engineering Safety Center. The author thanks the following for extended technical discussions, providing data and technical papers, and/or timely response in the processing of test rollers:

J. Zabinski	Army Research Laboratory
C. Beal	Everlube Products Company
M. Dugger	Sandia National Laboratories
S. Prasad	Sandia National Laboratories
G. Doll	The University of Akron
A. Korenyi-Both	Tribologix Inc.

Trade names and trademarks are used in this report for identification only. Their usage does not constitute an official endorsement, either expressed or implied, by the National Aeronautics and Space Administration

References

1. McClendon, M., "NIRSpec MSS Magnet Actuator Life Test Unit Wear Particle Evaluation", no report number, document obtained by Krantz, T., May 16, 2011
2. Authors unstated, "Micro Shutter Subsystem (MSS) Qualification Unit Test Report", JWST-RPT-013819, Rev. A, June 2010.
3. Krantz, T., Shareef, I, "Wear of Steel and Ti6Al4V Rollers in Vacuum", proceedings of the 41st Aerospace Mechanisms Symposium, also NASA TM-2012-217610, 2012.
4. Pellicciotti, J. (*submitted by*), "JWST NIRSpec Micro Shutter Subsystem", NESC-RP-11-00701, 2012.
5. Nishimura, Makoto, and Mineo Suzuki. "Solid-lubricated ball bearings for use in a vacuum—state-of-the-art." *Tribology International* 32, no. 11, 1999.
6. Pepper, S., "Research Note-Characterization of the Test Environment of JWST Roller Wear Evaluation at NASA-GRC", Aug. 1, 2011.
7. Johnson, K.L., **Contact Mechanics**, Cambridge University Press, 1985.
8. Kalker, J.J., "Rolling contact phenomena: linear elasticity", *Rolling Contact Phenomena CISM Courses and Lectures*, Issue 411, Springer-Verlag, 2000.
9. McGinness, H., "Lateral forces induced by a misaligned roller", DSN Progress Report 42-45, March and April 1978, Jet Propulsion Laboratory, Pasadena, Calif., 1978.
10. Krantz, T., DellaCorte, C., Dube, M., "Experimental Investigation of Forces Produced by Misaligned Steel Rollers", proceedings of the 40th Aerospace Mechanisms Symposium, NASA/CP-2010-216272, also NASA/TM-2010-216741, 2010.
11. Antoine, J. F., et al. "Approximate Analytical Model for Hertzian Elliptical Contact Problems." *Journal of Tribology* Vol. 128, 2006.
12. Archard, J. F., &Hirst, W. "The wear of metals under unlubricated conditions.", *Proceedings of the Royal Society of London. Series A. Mathematical and Physical Sciences*, Vol. 236, 1956
13. Roberts, E. W. "Space tribology: its role in spacecraft mechanisms." *Journal of Physics D: Applied Physics* 45, no. 50 , 2012.
14. Scharf, T. W., and S. V. Prasad. "Solid lubricants: a review." *Journal of Materials Science* 48, no. 2, 2013.
15. Authors not stated, "Properties of Du Pont VESPEL® Parts", Brochure Number H-15724-1, Du Pont Corporation, 1993.
16. Wheeler, J. M., C. A. Collier, J. M. Paillard, and J. A. Curran. "Evaluation of micromechanical behaviour of plasma electrolytic oxidation (PEO) coatings on Ti-6Al-4V." *Surface and Coatings Technology* 204, no. 21, 2010..
17. Santos, Lucia V., Vladimir J. Trava-Airoldi, Evaldo J. Corat, JadirNogueira, and Nélia F. Leite. "DLC cold welding prevention films on a Ti6Al4V alloy for space applications." *Surface and Coatings Technology* 200, no. 8, 2006.
18. Eckels, M., M. N. Kotzalas, and G. L. Doll. "Attaining High Levels of Bearing Performance with a Nanocomposite Diamond-Like Carbon Coating." *Tribology Transactions* 56, no. 3, 2013.
19. Scharf, T. W., P. G. Kotula, and S. V. Prasad. "Friction and wear mechanisms in MoS₂/Sb₂O₃/Au nanocomposite coatings." *Acta Materialia* 58, no. 12, 2010.

